JCI The Journal of Clinical Investigation

T cell–mediated vascular dysfunction of human allografts results from IFN-γ dysregulation of NO synthase

Kian Peng Koh, Yinong Wang, Tai Yi, Stephen L. Shiao, Marc I. Lorber, William C. Sessa, George Tellides, Jordan S. Pober

J Clin Invest. 2004;114(6):846-856. https://doi.org/10.1172/JCI21767.

Article **Cardiology**

Allograft vascular dysfunction predisposes to arteriosclerosis and graft loss. We examined how dysfunction develops in transplanted human arteries in response to circulating allogeneic T cells in vivo using immunodeficient murine hosts. Within 7–9 days, transplanted arteries developed endothelial cell (EC) dysfunction but remained sensitive to exogenous NO. By 2 weeks, the grafts developed impaired contractility and desensitization to NO, both signs of VSMC dysfunction. These T cell–dependent changes correlated with loss of eNOS and expression of iNOS — the latter predominantly within infiltrating T cells. Neutralizing IFN-γ completely prevented both vascular dysfunction and changes in NOS expression; neutralizing TNF reduced IFN-γ production and partially prevented dysfunction. Inhibiting iNOS partially preserved responses to NO at 2 weeks and reduced graft intimal expansion after 4 weeks in vivo. In vitro, memory $CD4^+$ T cells acted on allogeneic cultured ECs to reduce eNOS activity and expression of protein and mRNA. These effects required T cell activation by class II MHC antigens and costimulators (principally lymphocyte function-associated antigen–3, or LFA-3) on the ECs and were mediated by production of soluble mediators including IFN-γ and TNF. We conclude that IFN-γ is a central mediator of vascular dysfunction and, through dysregulation of NOS expression, links early dysfunction with late arteriosclerosis.

Find the latest version:

https://jci.me/21767/pdf

 Related Commentary, page 762

T cell–mediated vascular dysfunction of human allografts results from IFN-γ dysregulation of NO synthase

Kian Peng Koh,[1,2] Yinong Wang,[1,3] Tai Yi,[1,3] Stephen L. Shiao,[1,4] Marc I. Lorber,[1,3] William C. Sessa,[1,2] George Tellides,[1,3] and Jordan S. Pober[1,4,5]

[1]Interdepartmental Program in Vascular Biology and Transplantation, Boyer Center for Molecular Medicine, [2]Department of Pharmacology, [3]Department of Surgery, [4]Section of Immunobiology, and [5]Department of Pathology, Yale University School of Medicine, New Haven, Connecticut, USA.

Allograft vascular dysfunction predisposes to arteriosclerosis and graft loss. We examined how dysfunction develops in transplanted human arteries in response to circulating allogeneic T cells in vivo using immunodeficient murine hosts. Within 7–9 days, transplanted arteries developed endothelial cell (EC) dysfunction but remained sensitive to exogenous NO. By 2 weeks, the grafts developed impaired contractility and desensitization to NO, both signs of VSMC dysfunction. These T cell–dependent changes correlated with loss of eNOS and expression of iNOS — the latter predominantly within infiltrating T cells. Neutralizing IFN-γ completely prevented both vascular dysfunction and changes in NOS expression; neutralizing TNF reduced IFN-γ production and partially prevented dysfunction. Inhibiting iNOS partially preserved responses to NO at 2 weeks and reduced graft intimal expansion after 4 weeks in vivo. In vitro, memory CD4+ T cells acted on allogeneic cultured ECs to reduce eNOS activity and expression of protein and mRNA. These effects required T cell activation by class II MHC antigens and costimulators (principally lymphocyte function-associated antigen–3, or LFA-3) on the ECs and were mediated by production of soluble mediators including IFN-γ and TNF. We conclude that IFN-γ is a central mediator of vascular dysfunction and, through dysregulation of NOS expression, links early dysfunction with late arteriosclerosis.

Introduction

Posttransplant graft arteriosclerosis, the major cause of solid organ allograft failure, is characterized by rapidly progressive stenosis of graft conduit arteries, causing ischemic injury and replacement fibrosis in the graft parenchyma (1). Like other vascular diseases, structural changes of intimal hyperplasia and inward vascular remodeling (reduction in vessel circumference) contribute independently to lumen loss (2). In addition, functional abnormalities in vasoconstriction or vasodilatation, due to endothelial cell (EC) and/or VSMC dysfunction, may cause dynamic reductions in luminal diameter even before structural abnormalities develop (3). The alloantigen-dependent host anti-graft immune response contributes significantly to the development of structural lesions. However, both immune and nonimmune factors, including ischemia-reperfusion injury, cytomegalovirus infection, dyslipidemia, hypertension, and immunosuppressive agents, may contribute to graft vessel dysfunction (4). To this day, the pathophysiological mechanisms of graft dysfunction remain obscure, yet are important to understand since dysfunction is predictive of the development of graft arteriosclerosis and linked to an adverse clinical outcome (5, 6).

Under physiological conditions, arterial ECs regulate blood flow by releasing NO, prostaglandin I_2, and endothelium-derived hyperpolarizing factor, all of which relax the basal tone of VSMCs (7). NO, formed by Ca^{2+}-dependent conversion of L-arginine to NO and L-citrulline by eNOS, is the major regulator of tone in conduit arteries. Impaired synthesis of NO, a key mechanism in EC dysfunction, frequently occurs in inflammatory syndromes (8) and reduces the vasodilator response of blood vessels. On the other hand, proinflammatory cytokines can induce a second isoform of NOS — iNOS — in vascular tissue, especially in VSMCs and/or infiltrating leukocytes (9). iNOS is a Ca^{2+}-independent high-output producer of NO and has been implicated in host defense and pathological reactions, such as circulatory shock, rather than physiologic regulation. Dysregulation in the expression of NOS isoforms may thus contribute to both VSMC and EC dysfunction.

The role of T lymphocytes in initiating graft EC dysfunction is unknown. Host lymphocytes typically accumulate subjacent to the luminal endothelium very early after transplantation (10). Moreover, human graft ECs can activate allogeneic host T cells through direct presentation of foreign MHC molecules and costimulators. On human ECs, the most important costimulator is lymphocyte function-associated antigen–3 (LFA-3), which is constitutively expressed (11). We hypothesize that activated T cells, in turn, impair EC and/or VSMC function. This idea cannot be tested in conventional rodent transplant models because of fundamental differences between human and rodent ECs and VSMCs, both with regard to how they control blood pressure and how they interact with and respond to T cells (11). For example, rodent ECs do not express LFA-3. Here, we describe the novel use of an experimental transplant model to study the development of vascular dysfunction in human arterial grafts that encounter allogeneic leukocytes in vivo within murine surrogate hosts. We demonstrate that allogeneic T cells can directly induce vascular

Nonstandard abbreviations used: CIITA, class II transactivator; EC, endothelial cell; HUVEC, human umbilical vein EC; LFA-3, lymphocyte function-associated antigen–3; L-NAME, Nω-nitro-L-arginine methyl ester; $PGF_{2\alpha}$, prostaglandin $F_{2\alpha}$; PSS, physiological salt solution; ROS, reactive oxygen species; sGC, soluble guanylate cyclase.

Conflict of interest: The authors have declared that no conflict of interest exists.

Citation for this article: *J. Clin. Invest.* **114**:846–856 (2004). doi:10.1172/JCI200421767.

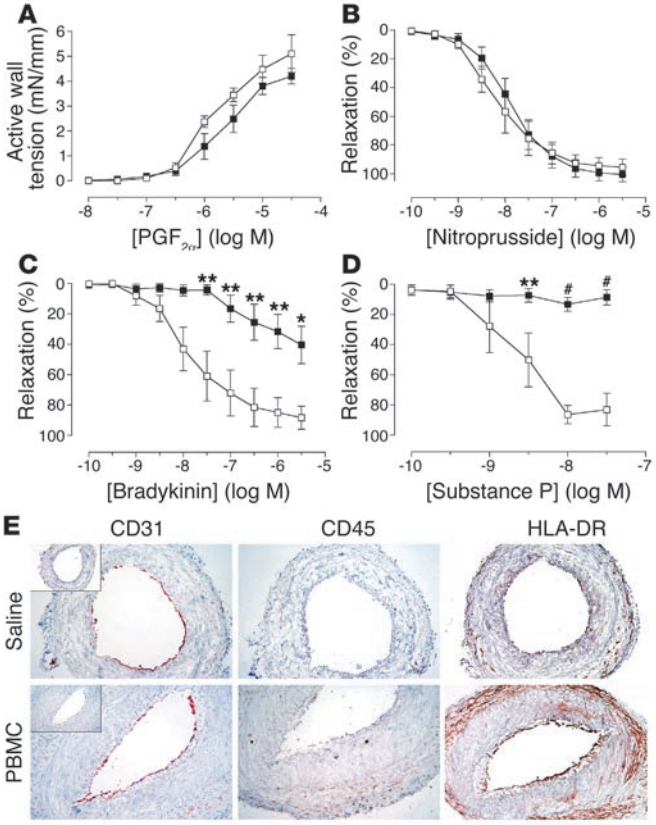

Figure 1
Effects of allogeneic T cells on arterial graft function at 1 week in vivo. Transplanted human arterial segments were recovered from mice injected with saline (open squares) or PBMCs (filled squares) 7–9 days before harvest (n = 5 pairs from four experiments). (**A**–**D**) Response curves. Restriction response to various concentrations of $PGF_{2\alpha}$ (**A**) and relaxation response curves for nitroprusside (**B**), bradykinin (**C**), or substance P (**D**) after preconstriction with $PGF_{2\alpha}$. $^{*}P < 0.05$; $^{**}P < 0.01$; $^{\#}P < 0.001$ vs. saline control. mN, milliNewtons. (**E**) Immunohistochemistry of graft sections stained for human and murine (inset) CD31, human CD45, and HLA-DR. The staining for human CD45 is indistinguishable from that for human CD3 (data not shown). Original magnification, ×200.

dysfunction, which begins in the ECs and then progresses to affect VSMCs. Dysfunction of both ECs and VSMCs is dependent upon the actions of the T cell–derived cytokine IFN-γ and results from dysregulation of the expression of NOS isoforms.

Results

Allogeneic T cells induce early graft endothelial dysfunction in vivo. Human coronary arterial segments interposed in the infrarenal aortae of immunodeficient SCID/beige mice have a normal histological appearance for up to 2 months (12). When recovered from the animals, these arterial grafts also displayed features of functional VSMCs and ECs, demonstrated by concentration-dependent constriction in response to the contractile agonist prostaglandin $F_{2\alpha}$ ($PGF_{2\alpha}$), and relaxation (following submaximal preconstriction) in response to the EC-independent NO donor sodium nitroprusside and the EC-dependent vasodilator bradykinin (Figure 1, A–C). Function was preserved for at least 5 weeks in control mice (data not shown). Inoculation of the mouse hosts with human PBMCs (allogeneic to the artery donor) resulted in circulating human leukocytes (consisting entirely of $CD3^+$ T cells and no $CD14^+$ monocytes) within a week (13), and infiltration of human T cells but not other leukocytes within the arterial grafts by 2 weeks. We investigated vasoreactivity of recovered grafts at 1–2 weeks after PBMC reconstitution, a time frame chosen to precede the development of structural remodeling of the grafts (12).

At 7–9 days after adoptive transfer of human PBMCs or saline (control) to the mouse recipients, five of six grafts from PBMC-injected mice (PBMC grafts) showed impaired relaxation responses to the EC-dependent agonists bradykinin (Figure 1C) and substance P (Figure 1D) compared with paired segments from control mice (saline grafts). However, both saline and PBMC grafts had similar concentration-dependent responses to $PGF_{2\alpha}$ (Figure 1A) and sodium nitroprusside (Figure 1B), suggesting that VSMC function remained intact and that dysfunction was restricted to ECs.

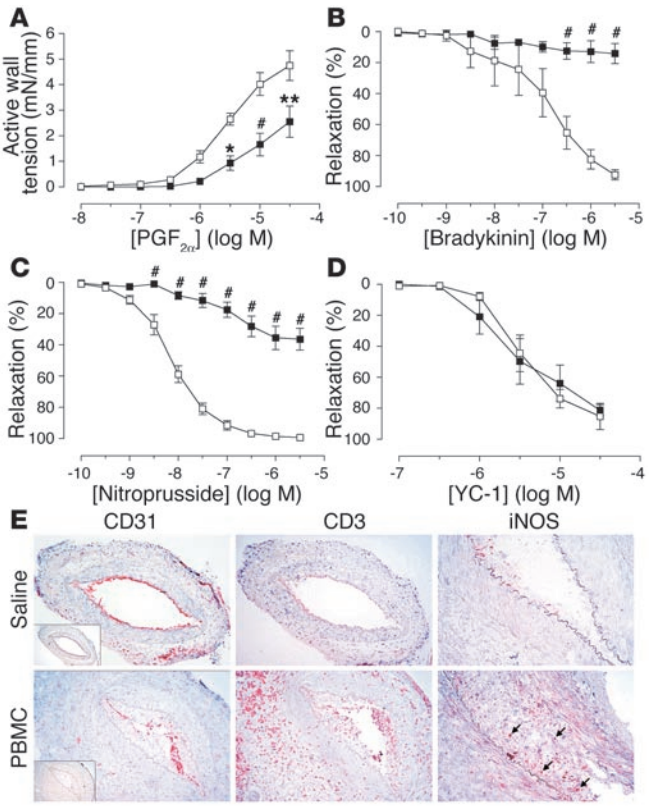

Figure 2
Effects of allogeneic T cells on arterial graft function at 2 weeks in vivo. Transplanted human arterial segments were recovered from mice injected with saline (open squares) or PBMCs (filled squares) for 13–15 days (n = 4–7 pairs from four to six experiments). (**A**–**D**) Response curves. Constriction response to various concentrations of $PGF_{2\alpha}$ (**A**) and relaxation response to bradykinin (**B**), nitroprusside (**C**), or YC-1 (**D**) after preconstriction with $PGF_{2\alpha}$. $^{*}P < 0.05$; $^{**}P < 0.01$; $^{\#}P < 0.001$ vs. saline control. (**E**) Immunohistochemistry of graft sections stained for human and murine (inset) CD31, human CD3, and iNOS. iNOS expression was highly localized to infiltrating T cells (arrows). Original magnification: CD31 and CD3 panels, ×200; iNOS panels, ×400.

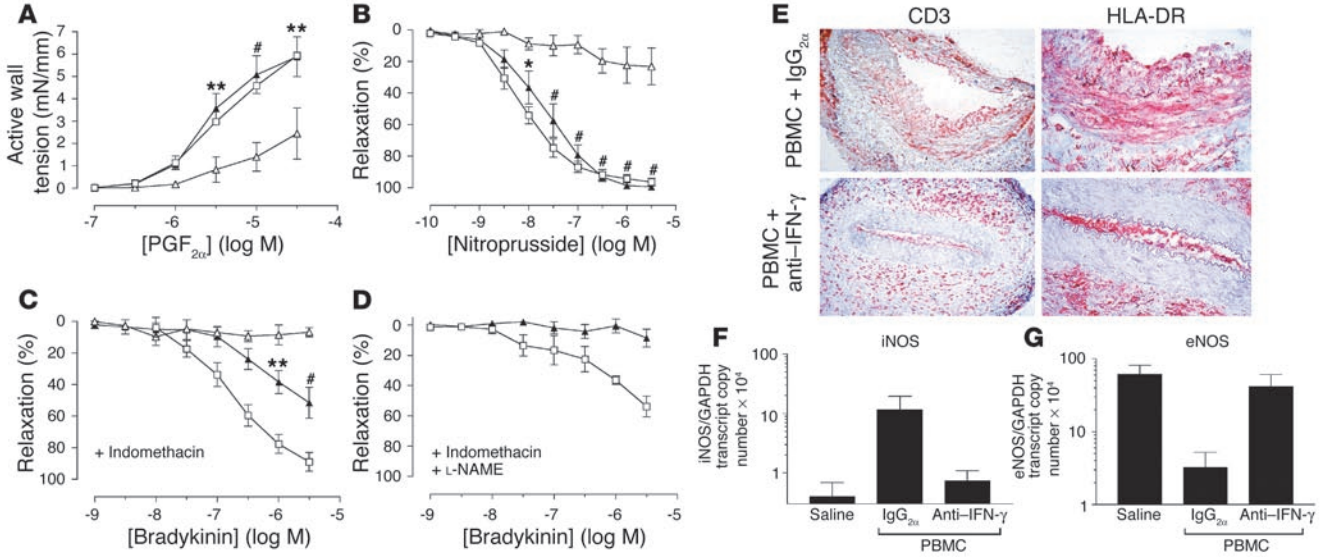

Figure 3

Effects of IFN-γ neutralization on T cell–mediated graft dysfunction in vivo. Transplanted human arterial segments were recovered from mice injected with saline alone (open squares) or PBMCs together with anti–IFN-γ mAb (filled triangles) or control mAb (IgG_{2a}) (open triangles) for 2 weeks (n = 5 matched triplicates from three experiments). (**A** and **B**) Endothelium-independent responses to various concentrations of $PGF_{2\alpha}$ (**A**) and nitroprusside (**B**). (**C** and **D**) Endothelium-dependent response to bradykinin before (**C**) and after (**D**) treatment with L-NAME. $^{*}P < 0.05$; $^{**}P < 0.01$; $^{\#}P < 0.001$ vs. PBMC + IgG_{2a} group, n = 3–5. (**E**) Immunohistochemistry of graft sections stained for human CD3 and HLA-DR. The luminal HLA-DR–positive cells are also human CD31–positive (data not shown). Goat anti-mouse secondary Ab alone did not stain the grafts. Original magnification: CD3 panels, ×200; HLA-DR panels, ×400. (**F** and **G**) RNA transcript levels of iNOS (**F**) and eNOS (**G**) in whole tissue sections analyzed by quantitative RT-PCR.

At this time point, PBMC grafts were generally indistinguishable in histological appearance from saline grafts (Figure 1E). Normal-appearing human endothelium, identified by species-specific CD31 staining (Figure 1E, left panels), lined the lumen of grafts in both groups. Human leukocytes were minimal or undetectable in the grafts by immunostaining (Figure 1E, middle panels). Saline grafts showed only minimal expression of HLA-DR, a human class II MHC antigen, representing a decline in expression caused by absence of human IFN-γ (a species-specific cytokine) in the mouse host (Figure 1E, upper right panel) (14). However, PBMC grafts showed enhanced expression of HLA-DR, predominantly localized to ECs lining the lumen and to cells in the adventitia (Figure 1E, lower right panel), indicative of IFN-γ–mediated activation (15).

Smooth muscle dysfunction follows EC dysfunction in arterial grafts. By 2 weeks (13–15 days) after PBMC injection, all arterial grafts examined showed an impaired contractility response to $PGF_{2\alpha}$ compared with saline controls (Figure 2A), indicative of the onset of VSMC dysfunction. When stimulated to similar preconstriction levels, PBMC grafts failed to relax when treated with bradykinin, indicative of continued EC dysfunction, whereas the paired saline grafts responded normally (Figure 2B). Remarkably, PBMC grafts at 2 weeks had also lost sensitivity to nitroprusside (Figure 2C). NO relaxes VSMCs by activating soluble guanylate cyclase (sGC) to convert GTP to cGMP. However, the NO-independent activator of sGC, YC-1 (16), relaxed both saline and PBMC grafts with similar potency (Figure 2D), suggesting that sGC was still active in these same grafts. Moreover, PBMC grafts could be maximally relaxed with the phosphodiesterase inhibitor papaverine (data not shown), confirming that the sGC-cGMP pathway remained functional.

At 2 weeks, PBMC grafts contained human $CD3^+$ T cells within the intimal and adventitial compartments (Figure 2E, middle panels). In addition, a few infiltrating T cells were now present in the media, although there was still no morphological evidence of VSMC injury or loss. The pattern of T cell infiltration suggests entry into the graft through both luminal ECs and adventitial microvascular ECs, without transmigration across the media. Some specimens displayed early evidence of intimal expansion; most showed focal loss of graft endothelium, but in all specimens, significant numbers of human $CD31^+$ ECs remained on the intimal surface (Figure 2E, left panels). iNOS was detectable in PBMC grafts but not saline grafts, and interestingly was highly localized to infiltrating T cells rather than VSMCs (Figure 2E, right panels).

T cell–derived IFN-γ is involved in dysregulation of NOS. We recently reported that blockade of IFN-γ prevented progressive stenosis that developed over 4 weeks in human arteries engrafted by the same procedure in PBMC-reconstituted SCID/beige mice (12). Here, we investigated whether IFN-γ also contributes to T cell–dependent graft dysfunction. Mouse recipients of adjacent arterial segments, in groups of three, were treated with either saline (one animal) or PBMCs (two animals); PBMC-reconstituted mice were also administered a neutralizing mAb against human IFN-γ or a control Ab for 2 weeks. Ab injections did not significantly modulate the numbers of circulating $CD3^+$ human T cells in the mouse circulation (data not shown). However, IFN-γ neutralization completely protected the VSMC function in five of five PBMC grafts; contractility and relaxation responses to $PGF_{2\alpha}$ (Figure 3A) and nitroprusside (Figure 3B) were similar to those of saline-injected controls. In contrast, grafts from animals that received PBMCs with control Ab (PBMC + IgG_{2a}) were not pro-

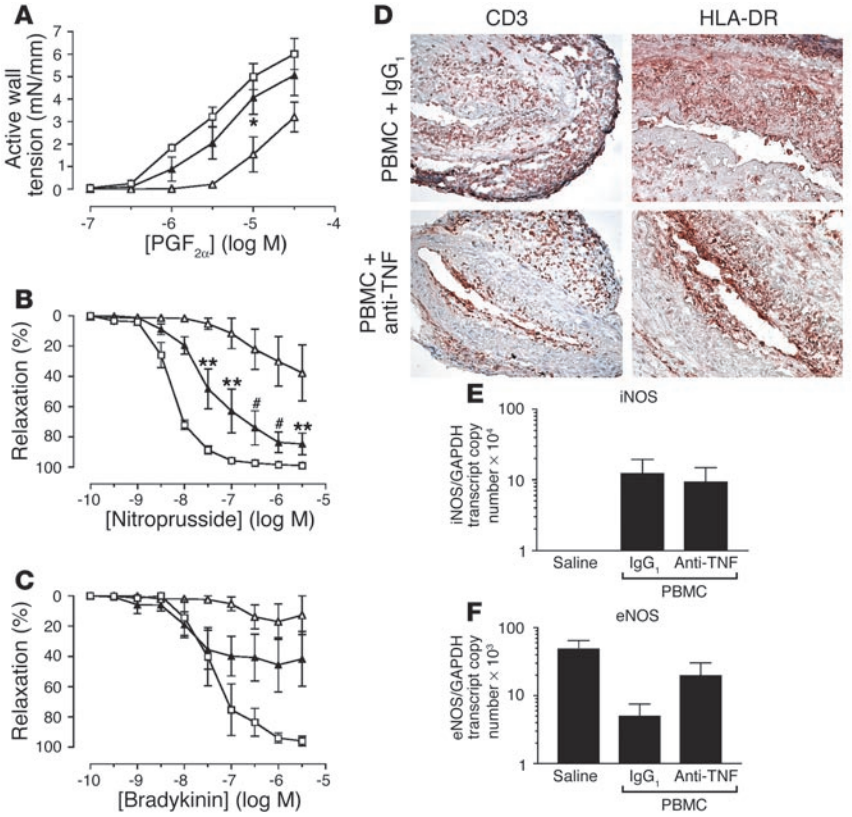

Figure 4
Effects of TNF neutralization on T cell–mediated graft dysfunction in vivo. Transplanted human arterial segments were recovered from mice injected with saline alone (open squares) or PBMCs together with anti-TNF mAb (filled triangles) or control mAb (IgG_1) (open triangles) for 2 weeks ($n = 4$ matched triplicates from two experiments). (**A**–**C**) Concentration-dependent responses to $PGF_{2\alpha}$ (**A**), nitroprusside (**B**), and bradykinin (**C**). $^{*}P < 0.05$; $^{**}P < 0.01$; $^{\#}P < 0.001$ vs. PBMC + IgG_1 group; $n = 3$–4. (**D**) Immunohistochemistry of graft sections stained for human CD3 and HLA-DR. Original magnification: CD3 panels, ×200; HLA-DR panels, ×400. (**E** and **F**) RNA transcript levels of iNOS (**E**) and eNOS (**F**) in whole tissue sections analyzed by quantitative RT-PCR.

tected. Anti–IFN-γ treatment also partially preserved EC-dependent relaxation by bradykinin (Figure 3C), a response completely blocked by treatment with the NOS inhibitor Nω-nitro-L-arginine methyl ester (L-NAME) in the presence of the cyclooxygenase inhibitor indomethacin (Figure 3D), indicating that the mediator of relaxation preserved by anti–IFN-γ treatment was NO, not endothelium-derived hyperpolarizing factor.

As noted earlier, PBMC grafts expressed HLA-DR predominantly on ECs and adventitial cells. By 2 weeks, we observed expression of this molecule, which was unaffected by control Ab injection, on VSMCs as well (Figure 3E, upper right panel). Anti–IFN-γ treatment abrogated HLA-DR expression on the VSMCs but not on luminal ECs and adventitial cells (Figure 3E, lower right panel). Significantly, $CD3^+$ T cells infiltrated PBMC grafts in similar numbers at 2 weeks despite anti–IFN-γ treatment (Figure 3E, left panels).

Quantitative analyses of messenger RNA encoding iNOS and eNOS isoforms in whole vessel sections revealed induction of iNOS in PBMC + IgG_{2a} grafts compared with saline grafts, although the degree of induction varied widely among different donors; IFN-γ neutralization abrogated this induction (Figure 3F). Conversely, eNOS transcripts were reduced in PBMC + IgG_{2a} grafts but preserved in PBMC + anti–IFN-γ grafts at a level comparable to that in saline grafts (Figure 3G). These data suggest that IFN-γ–dependent T cell alloresponses mediate vascular dysfunction by concomitant reduction of eNOS and induction of iNOS within the arterial wall.

TNF contributes partially to graft dysfunction. TNF reduces expression of eNOS in cultured ECs by mRNA destabilization (17) and also contributes to iNOS induction (18). To investigate the role of TNF in alloimmune-mediated graft dysfunction, we treated mouse graft recipients with PBMCs and anti–human TNF Ab. PBMC + anti-TNF grafts displayed improved contractility and EC-independent relaxation responses compared with PBMC + IgG_1 grafts (Figure 4, A and B), although the protection by anti-TNF was not as complete as observed with anti–IFN-γ. The PBMC + anti-TNF grafts also displayed a partial response to bradykinin that was primarily mediated by NO (Figure 4C and data not shown), although the difference from the PBMC + IgG_1 group did not reach statistical significance. Anti-TNF treatment did not prevent T cell infiltration or HLA-DR expression on graft ECs and medial VSMCs (Figure 4D). Moreover, iNOS expression was only mildly reduced, and eNOS expression partially preserved, by this treatment (Figure 4, E and F). Together, these data suggest that while TNF may contribute to T cell–dependent graft dysfunction, its effects are partial and redundant with other agents.

Table 1
Circulating human IFN-γ and TNF levels in PBMC-reconstituted mice[A]

	IFN-γ (pg/ml)	TNF (pg/ml)
PBMC + IgG_{2a} ($n = 5$)	512.9 ± 94.3	7.3 ± 1.7
PBMC + anti–IFN-γ ($n = 5$)	100.1 ± 85.3[B]	5.4 ± 2.2[C]
PBMC + IgG_1 ($n = 4$)	766.0 ± 229.6	5.9 ± 4.3
PBMC + anti-TNF ($n = 4$)	278.4 ± 119.6[D]	0.00

[A]Levels in saline-treated mice were undetectable (not shown). [B]$P < 0.05$ vs. PBMC + IgG_{2a}. [C]Not significant vs. PBMC + IgG_{2a}. [D]$P < 0.05$ vs. PBMC + IgG_1.

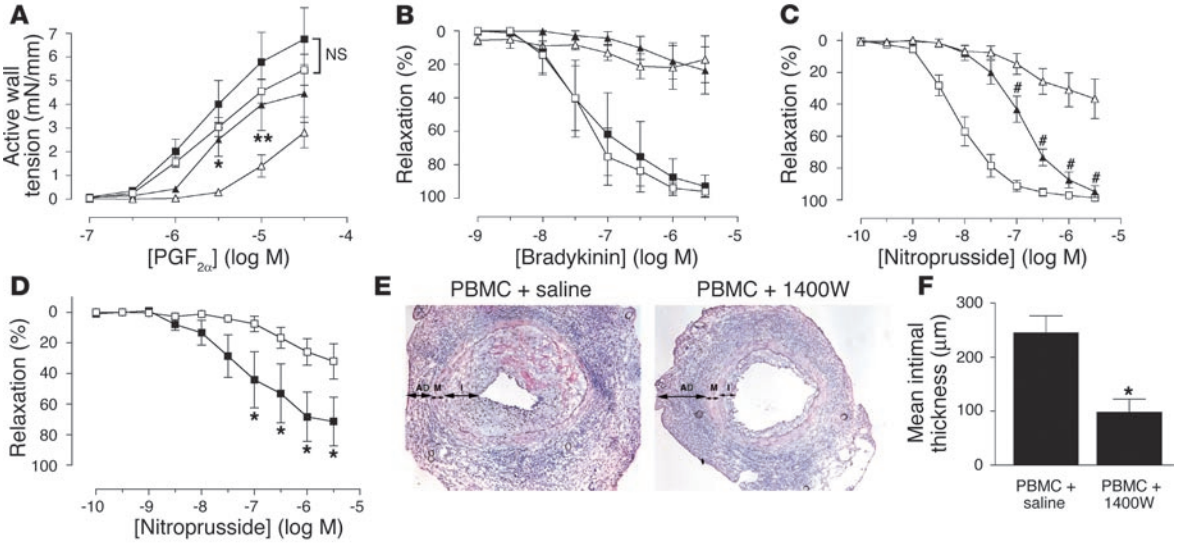

Figure 5
Contribution of iNOS to VSMC dysfunction and graft arteriosclerosis. (**A**–**C**) Arterial grafts recovered from animals at 2 weeks were exposed to the iNOS inhibitor 1400W ex vivo in the bath chamber (n = 3–6 pairs from four to five experiments). Concentration-dependent responses to $PGF_{2\alpha}$ (**A**), bradykinin (**B**), and nitroprusside (**C**) of grafts from saline (squares) and PBMC (triangles) groups were measured before (open symbols) and after (filled symbols) treatment with 1400W. *P < 0.05; **P < 0.01; #P < 0.001 vs. PBMC group before 1400W treatment. Treatment with 1400W did not cause significant changes in any response of the arteries harvested from saline-treated animals. Saline group after 1400W treatment is not shown in the nitroprusside response. (**D**) Arterial grafts were recovered from mice reconstituted with PBMCs and injected daily with saline (open squares) or 1400W (filled squares) for 2 weeks (n = 5 pairs from three experiments). Smooth muscle function was assessed by the relaxation response of preconstricted arteries to various concentrations of nitroprusside. (**E** and **F**) Paired arterial grafts recovered from mice reconstituted with PBMCs and injected daily with saline or 1400W for 4 weeks (n = 6 pairs from three experiments). Morphometry of H&E-stained tissue sections (**E**), in which compartments are demarcated as adventitia (AD), media (M), and intima (I), was analyzed to calculate mean intimal thickness (**F**). Original magnification: ×200.

In PBMC-injected mice, plasma levels of human IFN-γ typically reached 0.3–1.4 ng/ml by 2 weeks, and TNF levels were no higher than 20 pg/ml. With anti–IFN-γ treatment, human IFN-γ levels were significantly reduced to low or undetectable levels, but human TNF levels were not affected (Table 1). Interestingly, anti-TNF treatment not only neutralized TNF, but also significantly reduced IFN-γ (Table 1), suggesting that TNF may act indirectly by promoting T cell IFN-γ production.

iNOS contributes to VSMC dysfunction and graft arteriosclerosis. The dependence of iNOS expression on IFN-γ demonstrated in human arterial allografts suggests that human T cell–derived IFN-γ may mediate its potent biological effects through iNOS. Moreover, dysregulation of sGC has been proposed to arise from overexposure to NO (19), producing "desensitization" of VSMCs as shown in PBMC grafts at 2 weeks of treatment. We tested the connection between iNOS expression and desensitization of grafts to NO by exposing arterial grafts recovered from mice two weeks after introduction of allogenic PBMC to a specific inhibitor of iNOS, 1400W (20), in the bath chamber. The concentration of 1400W (10 μM) was able to inhibit human iNOS–derived NO production completely but had no effect on human eNOS activity in transfected COS-7 cells in vitro (unpublished data, K.P. Koh). Treating saline grafts with 1400W neither produced a significant change in contractility (Figure 5A) nor shifted the concentration-relaxation bradykinin response curve (Figure 5B), further indicating that the inhibitor had no effect on eNOS. Treating PBMC grafts with 1400W significantly, albeit incompletely, restored contractility in response to $PGF_{2\alpha}$ (Figure 5A) and also partially rescued the relaxation response to nitroprusside (Figure 5C), indicating that iNOS contributes to VSMC dysfunction. However, 1400W did not restore the response of PBMC grafts to bradykinin (Figure 5B), suggesting that EC dysfunction is separable from VSMC dysfunction and persists under blockade of iNOS activity.

iNOS-derived NO is a pleiotropic molecule, which reacts with multiple cellular targets (21). NO itself is known to inhibit VSMC proliferation (22) and protect against neointima formation (23, 24), but excessive NO can also react with superoxide to produce toxic peroxynitrite, which can cause vascular injury (25). We investigated the effect of iNOS inhibition on human allograft arteriosclerosis by administering 1400W in vivo to mice that received both human arterial and PBMC engraftment. At 2 weeks, chronic inhibition of iNOS by 1400W partially prevented VSMC dysfunction (Figure 5D), indicating that the dose of inhibitor was bioactive in vivo. When the treatment was prolonged to 4 weeks, at which time intimal expansion in PBMC allografts became evident, iNOS inhibition reduced intimal thickness significantly (Figure 5, E and F). These results suggest that in human allografts, T cell IFN-γ–induced iNOS expression contributes to both vascular dysfunction and graft arteriosclerosis. Moreover, they suggest that VSMC dysfunction is an important contributor to graft arteriosclerosis, since isolated EC dysfunction (in the presence of 1400W) is not sufficient to cause intimal expansion.

$CD4^+$ T cells downregulate eNOS in cultured ECs in vitro. Our in vivo studies suggest that allogeneic T cells mediate graft EC dysfunction by reducing eNOS expression in an IFN-γ–dependent manner. Reduction in eNOS transcript in PBMC grafts compared with

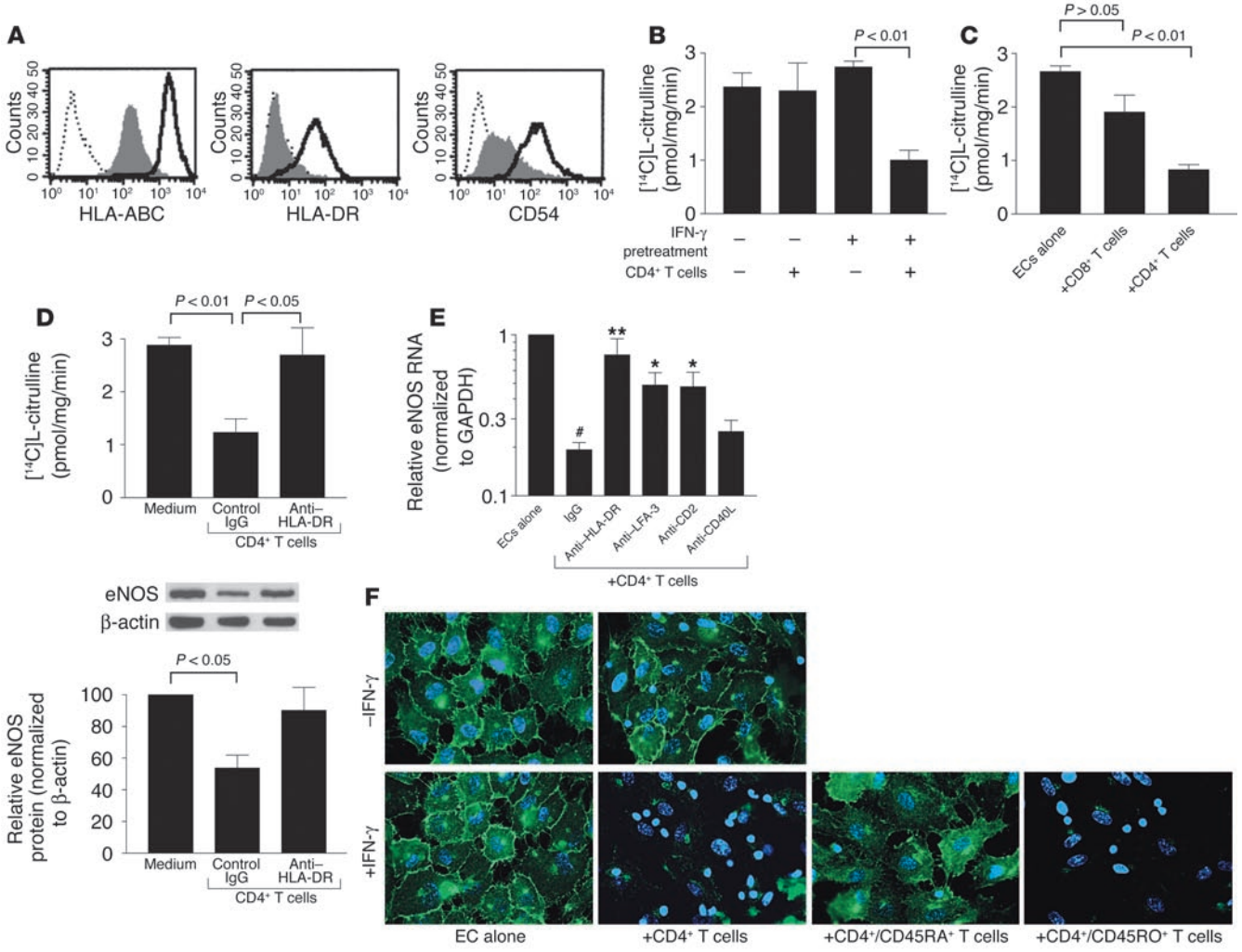

Figure 6

CD4+ memory T cells downregulate eNOS in class II MHC–positive ECs in vitro. (**A**) Flow cytometry of resting (shaded) or IFN-γ–pretreated (bold line) HUVECs immunostained for surface class I MHC (HLA-ABC), class II MHC (HLA-DR), and ICAM-1 (CD54). Dotted line, IgG_1 control. (**B**) NOS activity of HUVECs, either untreated or pretreated with IFN-γ, after CD4+ T cell coculture. (**C**) NOS activity of IFN-γ–pretreated HUVECs after CD8+ or CD4+ T cell coculture. (**D**) NOS activity of IFN-γ–pretreated HUVECs after CD4+ T cell coculture with control or anti–HLA-DR mAb. Below: eNOS protein levels determined by Western blot and densitometry and normalized to levels of β-actin in arbitrary units. Data in **A**–**D** represent mean ± SEM from at least four experiments. (**E**) eNOS RNA levels in IFN-γ–pretreated HUVECs after CD4+ T cell coculture with control IgG, or inhibitory mAb against HLA-DR, LFA-3, CD2, and CD40L (CD154). Values were expressed relative to those of HUVECs alone. Isotype-matched IgG controls were pooled. Data represent mean ± SEM from five to eight experiments. #$P < 0.001$ vs. ECs alone; *$P < 0.01$ and **$P < 0.001$ vs. CD4+ T cell + IgG group. (**F**) Epifluorescence of eNOS cellular localization (green) with nuclei costaining (blue) in untreated or IFN-γ–pretreated HUVECs, cocultured with CD4+ T cells. IFN-γ–pretreated HUVECs were also cocultured with subsets of CD4+/CD45RA+ (naive) cells and CD4+/CD45RO+ (memory) cells. The smaller nuclei belong to T cells. Images are representative of three experiments. All cocultures were incubated for 3 days.

paired saline grafts occurred as early as day 7–9 following injection of PBMC (data not shown), whereas iNOS transcript induction was evident in PBMC grafts only at 2 weeks. Although high-output iNOS-derived NO can be a negative feedback regulator of eNOS activity and expression (26, 27), our results suggest that EC dysfunction can occur prior to and independent of iNOS induction. To confirm this conclusion, we performed in vitro coculture studies of purified human CD4+ or CD8+ T cells with allogeneic human umbilical vein ECs (HUVECs). Resting HUVECs express sufficient class I MHC to stimulate CD8+ T cells to proliferate (28), but IFN-γ pretreatment is necessary to restore in HUVECs class II MHC (HLA-DR) expression and the capacity to activate CD4+ T cells (29). IFN-γ also upregulates class I MHC molecules and ICAM-1 (Figure 6A). Both CD8+ and CD4+ responses are restricted to memory T cells (CD45RO+) and depend on costimulation provided largely by EC LFA-3 interacting with T cell CD2 (28, 29). In general, CD4+ T cells react more vigorously than CD8+ T cells and produce more cytokines (30).

We examined how T cells affected NO production in ECs by measuring NOS activity in ECs isolated from the cocultures. Cultured HUVECs are incapable of iNOS expression in the presence of proinflammatory cytokines (31) or T cells (data not shown), allowing us to study T cell effects on eNOS independent of iNOS. Although IFN-γ pretreatment did not on its own reduce (and often

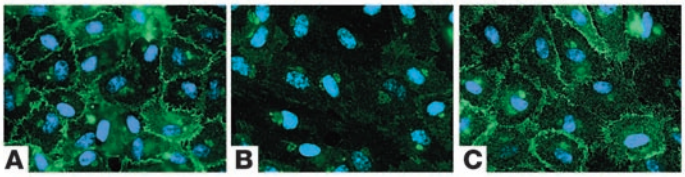

Figure 7
Contact dependence of EC response to T cells. Epifluorescence of eNOS immunostaining (green) with nuclei costaining (blue) of HUVECs that were pretreated with IFN-γ for 3 days prior to coculture with CD4+ T cells separated by a transwell. (**A**) ECs and T cells were cocultured in the absence of contact. (**B**) ECs below a transwell containing T cells in contact with IFN-γ–pretreated ECs. (**C**) ECs below a transwell containing T cells in contact with untreated (resting) ECs.

increased) NOS activity in HUVECs, it was required to reduce activity through coculture with CD4+ T cells (Figure 6B). In contrast, CD8+ T cells had no effect on NOS activity in resting HUVECs (data not shown), and were less potent than CD4+ T cells at reducing NOS activity in IFN-γ–pretreated HUVECs (Figure 6C). The reduction in NOS activity caused by CD4+ T cells was related to reduced eNOS protein and RNA expression, which could be restored by blocking HLA-DR recognition by the T cells (Figure 6, D and E). The reduction of eNOS RNA was also blocked by interfering with interactions between CD2 and LFA-3, but appeared to be independent of CD40L signals from CD4+ T cells (Figure 6E).

Immunofluorescence shows eNOS to be localized to the plasmalemma and Golgi (perinuclear) compartments of HUVECs (32). Expression in resting (IFN-γ–untreated) HUVECs was unaffected by coculture with CD4+ T cells. Expression was either unchanged or slightly increased in IFN-γ–pretreated HUVECs but was diminished with the addition of CD4+ T cells (Figure 6F). The CD4+ T cell effect on eNOS was primarily mediated by memory (CD45RO+) rather than naive (CD45RA+) cells (Figure 6F). These results suggest that CD4+ memory T cells, once activated by allogeneic ECs expressing class II MHC (which is IFN-γ dependent) and costimulator (principally LFA-3), reduce the capacity of ECs for NO production by diminishing expression of eNOS RNA and protein.

The reduction in eNOS expression in ECs cocultured with CD4+ T cells required contact between the two cell types, since separating T cells from IFN-γ–pretreated ECs using a transwell membrane prevented the effects on ECs (Figure 7A). To determine whether contact is involved only in T cell activation or is also required for the downregulation of eNOS in ECs, we cocultured ECs with CD4+ T cells above a cell-impermeable transwell and determined whether soluble factors released by EC-activated T cells can still affect a second monolayer of ECs cultured below the filter. Cocultures of T cells activated by IFN-γ–treated ECs caused eNOS expression to decrease in ECs across the transwell (Figure 7B). This effect did not require prior treatment of the second layer of ECs with exogenous IFN-γ (data not shown). In contrast, nonactivated cocultures of CD4+ T cells and resting (untreated) ECs had no effect on eNOS expression in ECs across the transwell (Figure 7C). Conditioned media collected from activated CD4+ T cell/EC cocultures also reduced eNOS expression in ECs, but the magnitude of reduction was variable (unpublished data, K.P. Koh). These results suggest that the release of soluble factors by T cells is sufficient to cause ECs to lose eNOS expression, but that some soluble factor(s) may be labile.

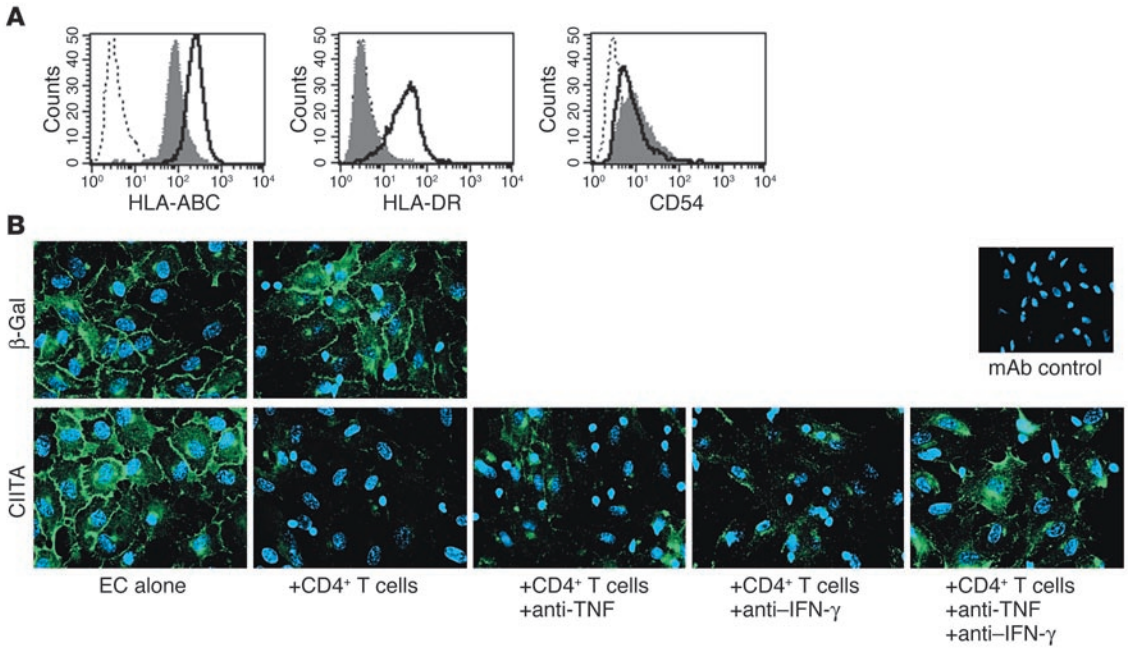

Figure 8
IFN-γ and TNF act in concert to reduce eNOS expression. (**A**) Flow cytometry of HUVECs transduced with β-gal (shaded) or class II transactivator (bold line) and stained for surface class I MHC (HLA-ABC), class II MHC (HLA-DR), and ICAM-1 (CD54). (**B**) Epifluorescence of eNOS cellular localization (green) with nuclei costaining (blue) in β-gal– or CIITA-transduced HUVECs cocultured for 3 days with CD4+ T cells. CIITA-transduced HUVECs were also cocultured with CD4+ T cells in the presence of anti-TNF and anti–IFN-γ mAb alone or in combination. mAb control: HUVEC cultures treated with both anti-TNF and anti–IFN-γ mAb and stained with secondary Ab only. Images are representative of five experiments.

To examine whether IFN-γ is one of the soluble factors with direct effects on eNOS, we used class II transactivator–transduced (CIITA-transduced) HUVECs, which express HLA-DR constitutively, independent of exogenous IFN-γ treatment and without other activation characteristics such as ICAM-1 expression (Figure 8A). When cocultured with allogeneic $CD4^+$ T cells, CIITA-transduced HUVECs displayed reduced eNOS expression (Figure 8B), whereas control ECs (transduced with β-gal) retained eNOS expression. Neutralizing both TNF and IFN-γ in the cocultures was more effective at preserving eNOS expression in CIITA-transduced HUVECs than neutralizing either cytokine alone (Figure 8B), suggesting possible interactions between IFN-γ and TNF. In these cocultures, the activated $CD4^+$ T cells produced up to 4 ng/ml of IFN-γ but only 50 pg/ml of TNF. Exogenous TNF reduced eNOS in HUVECs only at concentrations above 1 ng/ml, and IFN-γ did not significantly potentiate this effect in the absence of T cells (data not shown). Thus, while IFN-γ and TNF contribute to downregulation of eNOS in T cell/EC cocultures, they are not sufficient to explain the entire effect.

Discussion

Most experimental models of allograft vasculopathy have used orthotopic aortic transplantation or heterotopic grafting of whole hearts in rodents and swine (1), with insights derived largely through histologic and morphometric analyses of arterial intimal lesions. In contrast, few studies have examined vasomotor function of graft arteries. In one such investigation, rat aorta allografts performed across a minor histocompatibility barrier developed EC dysfunction (33), although VSMC loss due to medial necrosis developed quickly in this model. Heterotopic heart transplantation in swine also resulted in graft coronary EC dysfunction following acute rejection (34). While these models support a potential contribution of alloimmunity to EC dysfunction, it remains unresolved what immune effector mechanisms are involved. Moreover, alloimmunity in nonprimate species differs in significant ways from that of humans, making it difficult to extrapolate the information derived from studies of animal grafts to the clinical setting (11).

We used a human/mouse chimeric transplant model to define mechanisms of vascular dysfunction in human arterial grafts. In this model, arterial transplantation in an immunodeficient environment was performed 1 week prior to reconstitution of the host with human lymphoid cells. This strategy dissociates nonimmune injurious insults during transplantation, particularly ischemia-reperfusion injury, from subsequent immune mechanisms. Our results demonstrate that transplantation itself did not induce vascular dysfunction or enhance graft immunogenicity. Rather, the presence of human immune cells, consisting predominantly of T cells in our model, was necessary to cause graft dysfunction.

Various studies in cardiac transplant patients have correlated coronary EC dysfunction to elevated cytokine levels (35, 36) and attributed the dysfunction to reduced NO bioavailability (3, 37) and loss of eNOS in luminal ECs (38). In an apparent paradox, other studies have described elevated NO production in cardiac allografts associated with iNOS expression (39, 40). The constraints upon human investigation make it difficult to assess the sequelae of NOS alterations in the clinical setting. In our human artery model, we observed changes in both eNOS and iNOS expression that recapitulate the clinical observations. Moreover, our study demonstrates that EC dysfunction can occur prior to significant T cell infiltration and is temporally separable from subsequent iNOS expression and high-output NO production in human arterial grafts. In contrast, porcine coronary arteries in heterotopic cardiac grafts developed EC dysfunction but did not express iNOS within the study period (34). This may be because porcine arteries differ from rodent and human arteries in the mechanism of iNOS induction by cytokines (41) and underscores the importance of our studies on human specimens.

Among inflammatory leukocytes, macrophages are thought to be the predominant source of iNOS. However, mononuclear phagocytes do not engraft in SCID/beige mice following injection of human PBMCs (13, 14). Instead, we observed that the dominant iNOS-expressing cells in PBMC grafts were infiltrating human $CD3^+$ T cells. iNOS expression has been demonstrated in murine Th1 clones (42) and in T cells found within atheromas of cholesterol-fed rabbits (43). In several pilot experiments, we have not been able to induce iNOS in isolated human T cells cocultured with allogeneic human ECs and/or VSMCs, much in the same way that it has been difficult to induce iNOS in human monocytes or macrophages in vitro (44). The signals that regulate iNOS expression in human T cells may be species-specific and will require further investigation.

Our model demonstrates that iNOS induction resulted in impaired contractility and desensitization of VSMCs to NO. This phenomenon was partially reversible by 1400W, suggesting functional antagonism by excessive NO. We also considered the possibility that our observed VSMC dysfunction, particularly the desensitization to NO, may be caused by oxidative degradation of NO by reactive oxygen species (ROS). However, application of cell-permeable polyethylene glycol–superoxide dismutase to recovered PBMC grafts did not restore any response to nitroprusside (K.P. Koh, unpublished data). Moreover, the agent YC-1 is superoxide-sensitive (16), yet had similar dose responses on saline and PBMC grafts. Our present study does not rule out involvement of ROS in early vascular dysfunction, but suggests that iNOS-mediated desensitization of sGC is the major mechanism.

Previous studies in rodent allograft models have demonstrated a protective role of iNOS in suppressing intimal expansion (23, 24). In contrast, our studies in human allograft arteries demonstrate that iNOS promotes arteriosclerosis. The discrepancy of our results with those observed in rodents may result from differences in the biological actions of iNOS-derived NO in different species and experimental models. In particular, chronic rejection in the murine cardiac allograft model, in which recipient iNOS deficiency exacerbated graft arteriosclerosis, relied on T cell–depleting immunosuppression (24). In contrast, neointima formation in our model is T cell–mediated and therefore may have a different dependence on iNOS.

Multiple cytokines, including TNF, IFN-γ, and IL-1, are known to regulate iNOS in rodent tissues. Our study demonstrated that inhibiting IFN-γ by itself was sufficient to prevent iNOS expression and VSMC dysfunction in human arterial grafts. Surprisingly, we found that IFN-γ is also a central mediator of EC dysfunction involving loss of eNOS in vivo and in vitro. Many studies have focused on TNF as the key cytokine mediating EC dysfunction (45, 46), particularly because of its known effects on eNOS message stability. However, TNF did not fully account for eNOS downregulation in patients with severe heart failure (47). Our studies identify IFN-γ as an additional factor regulating eNOS. In clinical trials, anti-TNF therapy has been reported to improve

endothelial function in patients with rheumatoid arthritis and advanced heart failure (48, 49). In our study, we observed that (a) circulating IFN-γ was detected at much higher levels than TNF; (b) anti–IFN-γ completely prevented vascular dysfunction, but anti-TNF had only a partial effect; and (c) inhibiting TNF resulted in reduced IFN-γ production. These results suggest that anti–IFN-γ therapy may be more effective than anti-TNF in the treatment of vascular dysfunction.

In murine cardiac allograft models, IFN-γ deficiency protected allografts from vasculopathy by reducing expression of MHC antigens and leukocyte adhesion molecules (50, 51). In our model, anti–IFN-γ treatment for 2 weeks did not overtly reduce T cell infiltration or induction of class II MHC in the graft endothelium and adventitia, consistent with the previous finding that ECs are especially sensitive to IFN-γ (52). Yet the treatment protected against graft dysfunction, suggesting that IFN-γ is involved in changes other than T cell recruitment and activation. We propose a dual function for IFN-γ in the induction of graft vascular dysfunction. First, IFN-γ is needed to sustain class II MHC expression in graft endothelium. The source of IFN-γ may be basal levels in the circulation or allogeneic $CD8^+$ T cells that encounter constitutive class I MHC on graft ECs (53). The expression of class II MHC allows ECs to activate $CD4^+$ memory T cells, which secrete more IFN-γ. Second, IFN-γ directly contributes to dysregulation of NOS expression. Although IFN-γ by itself does not affect eNOS, it acts in concert with TNF and other factors to reduce eNOS expression and NO release by ECs. IFN-γ also has a central role in inducing iNOS within graft-infiltrating T cells. Finally, IFN-γ–dependent iNOS induction in human T cells exacerbates neointima formation, providing a potential mechanistic link between vascular dysfunction and arteriosclerosis.

In conclusion, our studies suggest that IFN-γ is a central mediator of allogeneic T cell–induced dysfunction of transplanted human arteries operating through dysregulation of NO production. These effects add to the previously described involvement of IFN-γ in intimal expansion and remodeling (12, 15), and further suggest that IFN-γ, through induction of iNOS, is a critical determinant linking early vascular dysfunction with later structural changes in graft arteriosclerosis. Our studies suggest that preservation of graft vascular function, by inhibiting IFN-γ synthesis and action, can lead to subsequent reduction of lumen loss.

Methods

Artery and PBMC engraftment. C.B-17 SCID/beige mice (Taconic Farms) were engrafted with size-matched adjacent segments (2–3 mm in length) of human coronary arteries devoid of visible atherosclerotic lesions and inoculated with human PBMCs or saline (vehicle control) 1 week later as previously described (12, 14). All protocols were approved by the Yale Human Investigations Committee and the Yale Animal Care and Use Committee.

Isometric tension measurement. Mice were sacrificed either approximately 1 week (days 7–9) or 2 weeks (days 13–15) after saline or PBMC injection and were perfused with physiological salt solution (PSS) containing 4 U/ml heparin through the left ventricle of the heart. The PSS was of the following composition: 118.3 mM NaCl, 4.7 mM KCl, 1.2 mM KH_2PO_4, 1.8 mM $CaCl_2$, 1.2 mM $MgCl_2$, 25 mM $NaHCO_2$, and 11.1 mM D(+)-glucose.

One arterial graft segment (1.2–2 mm long) was recovered within the suture lines from each mouse, carefully cleared of granulation tissue, and suspended as a ring in a 6-ml heated wire myograph bath chamber (Danish Myo Technology A/S) filled with PSS and bubbled with 95% O_2 and 5% CO_2 at a temperature of 37°C. Changes in isometric force were recorded on a multichannel digital interface (MyoDaq; Danish Myo Technology A/S). All experiments were performed in the presence of indomethacin (10 μM) to block the formation of vasoactive prostanoids.

The artery rings were equilibrated at a resting tension of 4–5 milliNewtons (mN) before constriction twice with an isotonic, maximally depolarizing potassium PSS (125 mM K^+ substituted for Na^+). The bath solution was changed back to the original PSS formula between stimulations. Contractility was assessed by a concentration response to $PGF_{2\alpha}$ (10 nM to 30 μM); active wall tension was expressed as force/(2 × segment length).

Endothelial function was assessed as the relaxation response to cumulative additions of bradykinin (1 nM to 3 μM) and/or substance P (0.1–30 nM) following preconstriction by $PGF_{2\alpha}$ to submaximal (EC_{50-70}) tone. Endothelium-independent relaxation was determined in a manner similar to the response to sodium nitroprusside (0.1 nM to 3 μM), YC-1 (0.1–30 μM; Alexis Biochemicals), or papaverine (300 μM). When comparing relaxation responses between treatment groups, care was taken to keep the developed tension at similar levels. NO production was inhibited by either 30 minutes of preincubation with the iNOS inhibitor 1400W (10 μM; Sigma-Aldrich) or 15 minutes of preincubation with the pan-NOS inhibitor L-NAME (300 μM). At the end of the experiments, the artery rings were removed from the tissue chamber and snap-frozen in TissueTek OCT (Sakura Finetek) for histological analyses. All chemicals were purchased from Sigma-Aldrich unless otherwise indicated. Experiments in which control vessels revealed dysfunction (less than 10% of total experiments) were excluded from analyses.

In vivo cytokine neutralization. Neutralizing mAb against human IFN-γ or human TNF (R&D Systems Inc.), or the respective IgG_{2a} (UPC-10) or IgG_1 (MOPC-21) isotype control mAb (Sigma-Aldrich), was injected subcutaneously at 250 μg into each mouse the day before PBMC injection and subsequently at 125 μg every 2–3 days for 2 weeks. At the time of sacrifice, retro-orbital blood was collected in EDTA. Plasma samples were frozen at –80°C until analysis for IFN-γ and TNF cytokine levels using sandwich ELISA kits (BioSource International) sensitive to 10 pg/ml and 0.5 pg/ml, respectively.

In vivo iNOS inhibition. Mice were injected subcutaneously with 10 mg/kg of 1400W (Sigma-Aldrich) daily starting from the day of PBMC injection. Arterial grafts were harvested either at 2 weeks for isometric tension measurement or 4 weeks for morphometric analysis as previously described (12). The intimal thickness, defined as the perpendicular distance between the luminal endothelium and the internal elastic lamina, was measured at four locations in each cross section by video microscopy, repeated for five cross sections, 150 μm apart, and averaged for each vessel.

Immunohistochemistry and tissue RNA analysis. Immunostaining was performed as described (14) using the following primary mAb's: mouse anti–human CD31, mouse anti–human HLA-DR (α-chain), and mouse anti–human CD45 (all from DAKO Corp.); mouse anti–human CD3 (R&D Systems Inc.); mouse anti-iNOS (Transduction Laboratories); and rat anti–mouse CD31 (BD Biosciences). Total RNA was isolated from frozen tissue sections and analyzed by quantitative real-time RT-PCR as previously described (12) using predeveloped TaqMan primers and probes for GAPDH iNOS (NOS2A), and eNOS (NOS3) (Assays-on-Demand; Applied Biosystems).

T cell and endothelial cell coculture. $CD4^+$ and $CD8^+$ T cells were isolated from cryopreserved PBMCs by positive selection using Ab-coated magnetic beads (Dynal Inc.). Purity of T cells was greater than 98% as assessed by FACS analysis. $CD4^+CD45RA^+$ and $CD4^+CD45RO^+$ cells were isolated by negative selection of $CD4^+$ T cells with anti-CD45RO and anti-CD45RA mAb (BioSource International), respectively. HUVECs were isolated, serially cultured as described (54), and used at passage three or four. Confluent EC monolayers were treated with or without 40 ng/ml human

IFN-γ (BioSource International) for 48–72 hours prior to addition of T cells. In some experiments, CIITA- or β-gal–transduced HUVECs, prepared by retroviral expression as described elsewhere (54), were substituted for IFN-γ–pretreated HUVECs. The ratio of T cells to ECs was in the range of 5:1 (in T25 flasks) to 10:1 (in C24 and C6 wells). Cocultures were performed for 3 days in Medium 199 supplemented with 20% FBS (Invitrogen Corp.) but excluding heparin and EC growth supplement. At the end of the coculture period, ECs were washed and suspended using trypsin-EDTA (Invitrogen Corp.). Residual lymphocytes were removed from the ECs using magnetic beads coated with anti-CD45 (Dynal Inc.). The ECs harvested by this procedure were viable (as verified by propidium iodide exclusion) and of ≥ 95% purity, determined by counting CD45-negative cells collected on a microscope slide by cytospin.

In vitro blocking Ab's. The blocking mAb's LB3.1 (anti–HLA-DR), TS2/9 (anti–LFA-3), TS2/18 (anti-CD2), and K16/16 (IgG_1 nonbinding control) were used as ascites preparations at saturating concentrations as previously described (29). The mAb's anti-CD40L (Beckman Coulter Inc.), anti–IFN-γ, anti-TNF, and isotype controls (R&D Systems Inc.) were used at 5–10 μg/ml.

NOS activity assay, Western blot, and RNA quantitation. Endogenous NOS activity was assayed by the conversion (inhibitable by 1 mM L-NAME) of [^{14}C]L-arginine to [^{14}C]L-citrulline in HUVEC lysates as previously described (55). NOS activity in HUVECs was fully Ca^{2+}-dependent (31). eNOS protein content in the lysates was quantified by Western blot and densitometry as described (32) using anti-eNOS (Transduction Laboratories) and anti–β-actin mAb (Sigma-Aldrich) as a loading control. Total RNA was isolated from HUVECs using a miniprep kit (QIAGEN Inc.) and analyzed by quantitative RT-PCR using TaqMan RT (Applied Biosystems) and iQ SYBR Green Supermix PCR (Bio-Rad Laboratories Inc.) reagents.

Immunofluorescence. HUVECs were plated on fibronectin-coated coverslips, pretreated as appropriate with IFN-γ, and cocultured with T cells as described above. In some experiments, T cells were separated from ECs using a semipermeable membrane with 0.4-μm pores (Falcon; BD Biosciences). Some transwells were further coated with fibronectin (BD Biosciences) and seeded with either IFN-γ–treated or untreated HUVECs for coculture with T cells in the upper chamber. After 3 days, cells were rinsed several times with PBS and immunostained for eNOS as described previously (32) using goat anti-mouse Alexa Fluor 488–conjugated secondary Ab (Molecular Probes Inc.); nuclei were counterstained with DAPI (Molecular Probes Inc.). Cells were analyzed by epifluorescence on an inverted Zeiss microscope. Z-series images were taken and merged after removal of out-of-focus information by Openlab deconvolution software (Improvision).

Statistics. Data are expressed as mean ± SEM. Comparisons were made using the Student's *t* test or ANOVA with the Bonferroni post-hoc test as appropriate. Differences were considered significant at $P < 0.05$.

Acknowledgments

This work was supported by NIH grant POI HL-70295-01; the Agency for Science, Research & Technology, Singapore (K.P. Koh); and the Medical Scientist Training Program (S.L. Shiao). We thank Nicholas Torpey, Ramona S. Scotland, and Gwendoline Davis for helpful laboratory assistance.

Received for publication March 31, 2004, and accepted in revised form July 13, 2004.

Address correspondence to: Jordan S. Pober, Yale University School of Medicine, 295 Congress Avenue, New Haven, Connecticut 06510, USA. Phone: (203) 737-2292; Fax: (203) 737-2293; E-mail: jordan.pober@yale.edu.

1. Libby, P., and Pober, J.S. 2001. Chronic rejection. *Immunity.* **14**:387–397.
2. Pethig, K., Heublein, B., Wahlers, T., and Haverich, A. 1998. Mechanism of luminal narrowing in cardiac allograft vasculopathy: inadequate vascular remodeling rather than intimal hyperplasia is the major predictor of coronary artery stenosis. Working Group on Cardiac Allograft Vasculopathy. *Am. Heart J.* **135**:628–633.
3. Fish, R.D., et al. 1988. Responses of coronary arteries of cardiac transplant patients to acetylcholine. *J. Clin. Invest.* **81**:21–31.
4. Tullius, S.G., and Tilney, N.L. 1995. Both alloantigen-dependent and -independent factors influence chronic allograft rejection. *Transplantation.* **59**:313–318.
5. Davis, S.F., et al. 1996. Early endothelial dysfunction predicts the development of transplant coronary artery disease at 1 year posttransplant. *Circulation.* **93**:457–462.
6. Hollenberg, S.M., et al. 2001. Coronary endothelial dysfunction after heart transplantation predicts allograft vasculopathy and cardiac death. *Circulation.* **104**:3091–3096.
7. Vanhoutte, P.M., and Mombouli, J.V. 1996. Vascular endothelium: vasoactive mediators. *Prog. Cardiovasc. Dis.* **39**:229–238.
8. Li, H., and Forstermann, U. 2000. Nitric oxide in the pathogenesis of vascular disease. *J. Pathol.* **190**:244–254.
9. Moncada, S., Palmer, R.M., and Higgs, E.A. 1991. Nitric oxide: physiology, pathophysiology, and pharmacology. *Pharmacol. Rev.* **43**:109–142.
10. Salomon, R.N., et al. 1991. Human coronary transplantation-associated arteriosclerosis. Evidence for a chronic immune reaction to activated graft endothelial cells. *Am. J. Pathol.* **138**:791–798.
11. Choi, J., Enis, D.R., Koh, K.P., Shiao, S.L., and Pober, J.S. 2004. T lymphocyte-endothelial cell interactions. *Annu. Rev. Immunol.* **22**:683–709.
12. Wang, Y., et al. 2004. Interferon-gamma plays a nonredundant role in mediating T-cell-dependent outward vascular remodeling of allogeneic human coronary arteries. *FASEB J.* **18**:606–608.
13. Pober, J.S., et al. 2003. Immunopathology of human T cell responses to skin, artery and endothelial cell grafts in the human peripheral blood lymphocyte/severe combined immunodeficient mouse. *Springer Semin. Immunopathol.* **25**:167–180.
14. Lorber, M.I., et al. 1999. Human allogeneic vascular rejection after arterial transplantation and peripheral lymphoid reconstitution in severe combined immunodeficient mice. *Transplantation.* **67**:897–903.
15. Tellides, G., et al. 2000. Interferon-gamma elicits arteriosclerosis in the absence of leukocytes. *Nature.* **403**:207–211.
16. Mulsch, A., et al. 1997. Effect of YC-1, an NO-independent, superoxide-sensitive stimulator of soluble guanylyl cyclase, on smooth muscle responsiveness to nitrovasodilators. *Br. J. Pharmacol.* **120**:681–689.
17. Yoshizumi, M., Perrella, M.A., Burnett, J.C., Jr., and Lee, M.E. 1993. Tumor necrosis factor downregulates an endothelial nitric oxide synthase mRNA by shortening its half-life. *Circ. Res.* **73**:205–209.
18. Busse, R., and Mulsch, A. 1990. Induction of nitric oxide synthase by cytokines in vascular smooth muscle cells. *FEBS Lett.* **275**:87–90.
19. De Kimpe, S.J., Van Heuven-Nolsen, D., van Amsterdam, J.G., Radomski, M.W., and Nijkamp, F.P. 1994. Induction of nitric oxide release by interferon-gamma inhibits vasodilation and cyclic GMP increase in bovine isolated mesenteric arteries. *J. Pharmacol. Exp. Ther.* **268**:910–915.
20. Garvey, E.P., et al. 1997. 1400W is a slow, tight binding, and highly selective inhibitor of inducible nitric-oxide synthase in vitro and in vivo. *J. Biol. Chem.* **272**:4959–4963.
21. Bogdan, C. 2001. Nitric oxide and the immune response. *Nat. Immunol.* **2**:907–916.
22. Garg, U.C., and Hassid, A. 1989. Nitric oxide-generating vasodilators and 8-bromo-cyclic guanosine monophosphate inhibit mitogenesis and proliferation of cultured rat vascular smooth muscle cells. *J. Clin. Invest.* **83**:1774–1777.
23. Shears, L.L., et al. 1997. Inducible nitric oxide synthase suppresses the development of allograft arteriosclerosis. *J. Clin. Invest.* **100**:2035–2042.
24. Koglin, J., Glysing-Jensen, T., Mudgett, J.S., and Russell, M.E. 1998. Exacerbated transplant arteriosclerosis in inducible nitric oxide-deficient mice. *Circulation.* **97**:2059–2065.
25. Villa, L.M., Salas, E., Darley-Usmar, V.M., Radomski, M.W., and Moncada, S. 1994. Peroxynitrite induces both vasodilatation and impaired vascular relaxation in the isolated perfused rat heart. *Proc. Natl. Acad. Sci. U. S. A.* **91**:12383–12387.
26. Buga, G.M., Griscavage, J.M., Rogers, N.E., and Ignarro, L.J. 1993. Negative feedback regulation of endothelial cell function by nitric oxide. *Circ. Res.* **73**:808–812.
27. Vaziri, N.D., and Wang, X.Q. 1999. cGMP-mediated negative-feedback regulation of endothelial nitric oxide synthase expression by nitric oxide. *Hypertension.* **34**:1237–1241.
28. Epperson, D.E., and Pober, J.S. 1994. Antigen-presenting function of human endothelial cells. Direct activation of resting CD8 T cells. *J. Immunol.* **153**:5402–5412.
29. Savage, C.O., Hughes, C.C., McIntyre, B.W., Picard, J.K., and Pober, J.S. 1993. Human CD4+ T cells proliferate to HLA-DR+ allogeneic vascular endothelium. Identification of accessory interac-

tions. *Transplantation.* **56**:128–134.
30. Doukas, J., and Pober, J.S. 1990. Lymphocyte-mediated activation of cultured endothelial cells (EC). CD4+ T cells inhibit EC class II MHC expression despite secreting IFN-gamma and increasing EC class I MHC and intercellular adhesion molecule-1 expression. *J. Immunol.* **145**:1088–1098.
31. Rosenkranz-Weiss, P., et al. 1994. Regulation of nitric oxide synthesis by proinflammatory cytokines in human umbilical vein endothelial cells. Elevations in tetrahydrobiopterin levels enhance endothelial nitric oxide synthase specific activity. *J. Clin. Invest.* **93**:2236–2243.
32. Fulton, D., et al. 2002. Localization of endothelial nitric-oxide synthase phosphorylated on serine 1179 and nitric oxide in Golgi and plasma membrane defines the existence of two pools of active enzyme. *J. Biol. Chem.* **277**:4277–4284.
33. Andriambeloson, E., et al. 2001. Transplantation-induced endothelial dysfunction as studied in rat aorta allografts. *Transplantation.* **72**:1881–1889.
34. Perrault, L.P., et al. 1997. Time course of coronary endothelial dysfunction in acute untreated rejection after heterotopic heart transplantation. *J. Heart Lung Transplant.* **16**:643–657.
35. Weis, M., et al. 1999. Modulation of coronary vasomotor tone by cytokines in cardiac transplant recipients. *Transplantation.* **68**:1263–1267.
36. Gullestad, L., et al. 1999. Possible role of proinflammatory cytokines in heart allograft coronary artery disease. *Am. J. Cardiol.* **84**:999–1003.
37. Weis, M., and Cooke, J.P. 2003. Cardiac allograft vasculopathy and dysregulation of the NO synthase pathway. *Arterioscler. Thromb. Vasc. Biol.* **23**:567–575.
38. Vejlstrup, N.G., Andersen, C.B., Boesgaard, S., Mortensen, S.A., and Aldershvile, J. 2002. Temporal changes in myocardial endothelial nitric oxide synthase expression following human heart transplantation. *J. Heart Lung Transplant.* **21**:211–216.
39. Ravalli, S., et al. 1998. Inducible nitric oxide synthase expression in smooth muscle cells and macrophages of human transplant coronary artery disease. *Circulation.* **97**:2338–2345.
40. Wildhirt, S.M., et al. 2001. Expression of endomyocardial nitric oxide synthase and coronary endothelial function in human cardiac allografts. *Circulation.* **104**(Suppl. 1):I336–I343.
41. Shibano, T., and Vanhoutte, P.M. 1993. Induction of NO production by TNF-alpha and lipopolysaccharide in porcine coronary arteries without endothelium. *Am. J. Physiol.* **264**:H403–H407.
42. Taylor-Robinson, A.W., et al. 1994. Regulation of the immune response by nitric oxide differentially produced by T helper type 1 and T helper type 2 cells. *Eur. J. Immunol.* **24**:980–984.
43. Esaki, T., et al. 1997. Expression of inducible nitric oxide synthase in T lymphocytes and macrophages of cholesterol-fed rabbits. *Atherosclerosis.* **128**:39–46.
44. Morris, S.M., Jr., and Billiar, T.R. 1994. New insights into the regulation of inducible nitric oxide synthesis. *Am. J. Physiol.* **266**:E829–E839.
45. Wang, P., Ba, Z.F., and Chaudry, I.H. 1994. Administration of tumor necrosis factor-alpha in vivo depresses endothelium-dependent relaxation. *Am. J. Physiol.* **266**:H2535–H2541.
46. Nakamura, M., et al. 2000. Effects of tumor necrosis factor-alpha on basal and stimulated endothelium-dependent vasomotion in human resistance vessel. *J. Cardiovasc. Pharmacol.* **36**:487–492.
47. Agnoletti, L., et al. 1999. Serum from patients with severe heart failure downregulates eNOS and is proapoptotic: role of tumor necrosis factor-alpha. *Circulation.* **100**:1983–1991.
48. Hurlimann, D., et al. 2002. Anti-tumor necrosis factor-alpha treatment improves endothelial function in patients with rheumatoid arthritis. *Circulation.* **106**:2184–2187.
49. Fichtlscherer, S., et al. 2001. Tumor necrosis factor antagonism with etanercept improves systemic endothelial vasoreactivity in patients with advanced heart failure. *Circulation.* **104**:3023–3025.
50. Nagano, H., et al. 1998. Coronary arteriosclerosis after T-cell-mediated injury in transplanted mouse hearts: role of interferon-gamma. *Am. J. Pathol.* **152**:1187–1197.
51. Nagano, H., et al. 1997. Interferon-γ deficiency prevents coronary arteriosclerosis but not myocardial rejection in transplanted mouse hearts. *J. Clin. Invest.* **100**:550–557.
52. Messadi, D.V., Pober, J.S., and Murphy, G.F. 1988. Effects of recombinant gamma-interferon on HLA-DR and DQ expression by skin cells in short-term organ culture. *Lab. Invest.* **58**:61–67.
53. Brooks, C.J., Stackpoole, A., and Savage, C.O. 1993. Synergistic interactions of CD4+ and CD8+ T cell subsets with human vascular endothelial cells in primary proliferative allogeneic responses. *Int. Immunol.* **5**:1041–1048.
54. Madge, L.A., Li, J.H., Choi, J., and Pober, J.S. 2003. Inhibition of phosphatidylinositol 3-kinase sensitizes vascular endothelial cells to cytokine-initiated cathepsin-dependent apoptosis. *J. Biol. Chem.* **278**:21295–21306.
55. Lin, M.I., et al. 2003. Phosphorylation of threonine 497 in endothelial nitric oxide synthase coordinates the coupling of L-arginine metabolism to efficient nitric oxide production. *J. Biol. Chem.* **278**:44719–44726.